



# Integro-Differential Analysis of Resonant Magnetic Metasurfaces With Equivalent Medium Approximation

I.V. Soares, F.M. Freitas, S.T.M. Gonçalves, U.C. Resende

## ► To cite this version:

I.V. Soares, F.M. Freitas, S.T.M. Gonçalves, U.C. Resende. Integro-Differential Analysis of Resonant Magnetic Metasurfaces With Equivalent Medium Approximation. IEEE Transactions on Magnetics, 2023, 59 (5), pp.7000704. <10.1109/TMAG.2023.3237163>. <hal-04123673>

**HAL Id: hal-04123673**

**<https://hal.science/hal-04123673v1>**

Submitted on 12 Jun 2023

**HAL** is a multi-disciplinary open access archive for the deposit and dissemination of scientific research documents, whether they are published or not. The documents may come from teaching and research institutions in France or abroad, or from public or private research centers.

L'archive ouverte pluridisciplinaire **HAL**, est destinée au dépôt et à la diffusion de documents scientifiques de niveau recherche, publiés ou non, émanant des établissements d'enseignement et de recherche français ou étrangers, des laboratoires publics ou privés.



Distributed under a Creative Commons CC BY-NC 4.0 - Attribution - Non-commercial use - International License

# Integro-Differential Analysis of Resonant Magnetic Metasurfaces with Equivalent Medium Approximation

Icaro V. Soares<sup>1</sup>, Felipe M. Freitas<sup>2</sup>, Sandro T. M. Gonçalves<sup>2</sup>, and Úrsula C. Resende<sup>2</sup>

<sup>1</sup>IETR (l'Institut d'électronique et des technologies du numérique) UMR 6164, CNRS / Univ. Rennes, Rennes, France

<sup>2</sup>Federal Center for Technological Education of Minas Gerais, DEE - PPGEL, Belo Horizonte 30421-169, Brazil

This paper proposes a strategy to consider the dielectric effects in the thin-wire integro-differential formulation and applies it to analyzing microstrip metasurfaces that support magnetic resonances. These structures comprise a periodic arrangement of subwavelength unit cells; therefore, the thin-wire approximation can be applied to analyze them. However, the substrate is usually disregarded. This work achieves more accurate results with a homogeneous equivalent medium approximation considering the dielectric properties. Moreover, an experimental methodology is presented to validate this implementation for each device as well as for the complete system. The proposed formulation is numerically solved with the Method of Moments, and the results show close agreement with experimental data. Besides, it leads to a significant reduction in the computation time compared to a full-wave analysis, which makes this approach also compelling for designing inductive wireless power transfer systems and magnetic resonators.

**Index Terms**—Computational electromagnetism, integral equation, metamaterials, method of moments, wireless power transfer.

## I. INTRODUCTION

**R**ESONANT metasurfaces (MTS) are composed of a two-dimensional array of subwavelength unit cells, i.e., much smaller than the wavelength at its operating frequency. The unconventional behavior that arises from the interaction of the electromagnetic fields with these periodic artificial structures leads to the development of novel devices such as superlenses [1], frequency-selective structures, and electromagnetic cloaks [2]. For instance, MTSs that support magnetic resonances amplify the magnetic near-field in its vicinity [3] and, therefore, have been applied in Wireless Power Transfer (WPT) systems to increase the coupling between transmitter and receiver coils, enhancing the efficiency [1,4,5]. However, as MTSs comprise many unit cells, analyzing and synthesizing these structures are computationally costly. Moreover, particularly for WPT systems based on the magnetic resonance that operates at the frequency of a few MHz, these structures are physically large, making a three-dimensional full-wave simulation almost unfeasible.

Therefore, several formulations have been proposed in literature employing different approximations to speed up the analysis of these structures. First, WPT systems with MTS can be modeled as magnetically coupled circuits with their parameters calculated from geometrical dimensions based on quasi-static approximations [6,7]. Even though this approach is the fastest and provides a better physical insight into the system behavior, it may lead to significant deviations from measurement results, especially at frequencies in which the effects of the displacement current are considerable. More accurate results can be found with integro-differential formulations based on vector potentials. In this case, the thin-wire approximation is used to reduce the three-dimensional problem to a uni-dimensional analysis, which leads to precise results for filamentary structures. However, the dielectric medium

affects the behavior and resonant frequency of microstrip coils and MTS; therefore, the conventional formulation leads to inaccurate results. An alternative to take into account material media is applying stratified medium theory based on layered Green's functions [8]. Nevertheless, due to the mathematical complexity, it is an error-prone approach and significantly increases the computational cost.

Therefore, this work proposes a novel strategy to consider dielectric properties in the electromagnetic analysis of microstrip coils, MTSs, and resonators. In this case, the dielectric effects are considered by modeling the radiator immersed in a homogeneous equivalent medium according to the multipole Debye model. Besides, an experimental methodology is presented to meticulously validate the results obtained with this proposed approach solved with the Method of Moments. In this way, each device is individually analyzed, and the validity range of the proposed approach is established. Finally, the in-house code is applied to analyze a complete WPT system with a MTS, and the computed efficiency is compared to the measured values.

## II. ANALYSIS OF THIN MICROSTRIP STRUCTURES

### A. Problem Formulation

The problem under analysis consists of a resonant MTS composed of a two-dimensional array of subwavelength unit cells illuminated by the magnetic field generated by a microstrip loop, as shown in Fig. 1(a). In this analysis, the topology of the MTS and the source coil comprises Perfect Electric Conductor (PEC) loops etched on a substrate with relative electric permittivity  $\epsilon_r$  and tangent loss  $\tan \delta$ . Besides, a lumped capacitance  $C$  is included in each unit cell in order to tune its resonant frequency.

The magnetic MTS comprises thin microstrip lines in which the cross-section is much smaller than the wavelength  $\lambda$  at the resonant frequency  $f_r$ . Therefore, in this case, the problem can be understood as a thin-wire PEC structure with equivalent diameter  $a = \sqrt{(4w_f t_c)/\pi}$  which corresponds to a circular cross-section with the same area as the microstrip line

cross-section. This structure is considered as immersed in a homogeneous medium with an equivalent electric permittivity  $\varepsilon_{eq}$ , which is a function of the substrate properties, as shown in 1(b).

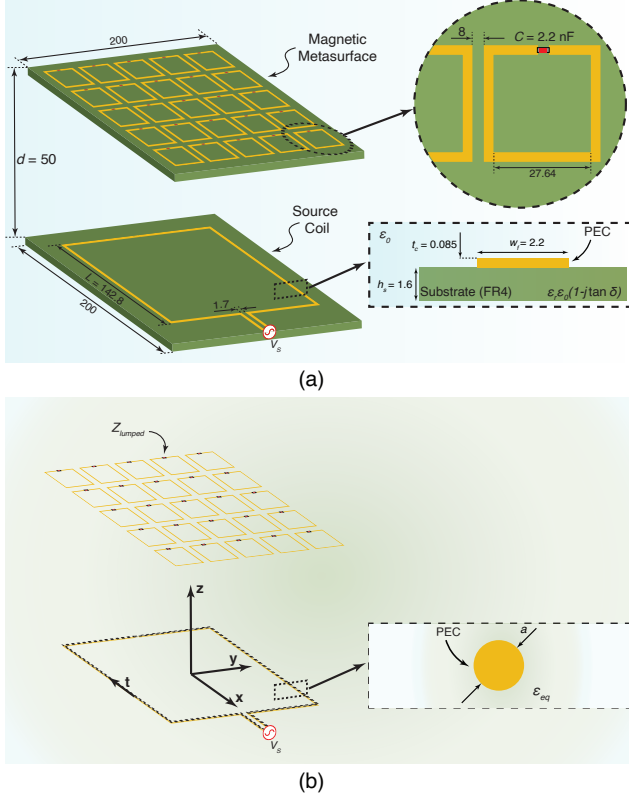


Fig. 1. Problem under analysis: (a) a magnetic metasurface composed of subwavelength unit cells is excited by the magnetic field produced by a microstrip source coil (all geometric dimensions in mm). In (b), an equivalent problem is proposed in which the microstrip structure is approximated by thin wires immersed in a homogeneous equivalent medium.

### B. Electromagnetic Modeling

A filamentary structure with arbitrary geometry in the tridimensional space  $\mathbb{R}^3$  can be modeled as a parametric function  $\mathbf{f}(t)$ . Therefore, the original structure defined in Cartesian coordinates  $[\mathbf{x}, \mathbf{y}, \mathbf{z}]$  can be analyzed as a unidimensional problem defined in the unit vector  $\mathbf{t}$  tangent to the curve  $\mathbf{f}(t)$ , as shown in Fig. 1(b).

In the problem under analysis, the diameter of the wire cross-section  $a \ll \lambda$ , and  $a \ll L$ , so the surface current density  $\mathbf{J}_s(\mathbf{r})$  can be approximated by a current that flows on the direction  $\mathbf{t}$  tangential to the wire, according to  $\mathbf{J}_s(\mathbf{r}') = I(t')/(2\pi a) \mathbf{t}$ . Consequently, the current  $\mathbf{I}(t')$  along the structure can be found by solving the integro-differential equation [9]:

$$\hat{\mathbf{n}} \times \mathbf{E}_{\text{inc}}(\mathbf{r}) = \hat{\mathbf{n}} \times \left[ \frac{j}{4\pi\omega\varepsilon_{eq}} \int_{t'} k^2 \mathbf{I}(t') \Psi(\mathbf{r}, \mathbf{r}') - [\nabla \cdot \mathbf{I}(t')] \nabla \Psi(\mathbf{r}, \mathbf{r}') dt' + Z_{\text{load}} \mathbf{I}(t') \right], \quad (1)$$

where  $\hat{\mathbf{n}}$  is the normal direction,  $\omega$  is the angular frequency,  $k$  is the wave propagation constant,  $\mathbf{E}_{\text{inc}}$  is the electric field incident to the structure,  $Z_{\text{load}}$  is the lumped impedance, and  $\Psi(\mathbf{r}, \mathbf{r}')$  is the Green's function given the position vector for the observer  $\mathbf{r}$  and source  $\mathbf{r}'$ . Henceforward, the apostrophe (') indicates quantities and operations related to the sources, while the others are related to the observer.

### C. Numerical Solution

The Eq. (1) is numerically solved by discretizing the geometry in  $N$  linear segments and then applying the Method of Moments (MoM). Therefore, the unknown current is expanded into a finite sum of  $N$  linear-piecewise basis functions  $\mathbf{u}_j(t') = u_j(t') \mathbf{t}'$ :  $\mathbf{I}(t') = \sum_{j=1}^N I_j \mathbf{u}_j(t')$ , where the unknown coefficients  $I_j$  can be determined by taking the inner product of (1) with the linear-piecewise weighting functions  $\mathbf{w}_j(t) = w_j(t) \mathbf{t}$  and integrating it over the observer segments [10]. In this way, (1) can be rewritten as a linear system of  $N$  equations, expressed in matrix form as  $\mathbb{V}_{(N \times 1)} = [\mathbb{Z}_{(N \times N)} + \mathbb{Z}_{(N \times N)}^{\text{load}}] \cdot \mathbb{I}_{(N \times 1)}$ , where the elements of the distributed  $\mathbb{Z}$  and lumped  $\mathbb{Z}^{\text{load}}$  impedance matrices are respectively given by:

$$\mathbb{Z}_{i,j} = \frac{j}{4\pi\omega\varepsilon_{eq}} \int_t \int_{t'} k^2 w_i(t) u_j(t') (\mathbf{t} \cdot \mathbf{t}') \Psi(\mathbf{r}, \mathbf{r}') - \frac{dw_i(t)}{dt} \frac{du_j(t')}{dt'} \Psi(\mathbf{r}, \mathbf{r}') dt' dt, \quad (2)$$

$$\mathbb{Z}_{i,j}^{\text{load}} = \int_t Z_{\text{load}} w_i(t) u_j(t') (\mathbf{t} \cdot \mathbf{t}') dt. \quad (3)$$

By modeling the incident field as  $\mathbf{E}_{\text{inc}}(\mathbf{r})$  as a delta-gap source, the elements of the excitation matrix  $\mathbb{V}$  are calculated as follows:

$$\mathbb{V}_i = \frac{V_S}{\Delta} \int_t w_i(t) dt, \quad (4)$$

where  $V_S$  is the voltage applied to the source coil and  $\Delta$  is the segment length.

### D. Proposed Equivalent Medium Approximation

Two media surround the microstrip line, the dielectric substrate, and the free space. An effective medium can be defined as a homogeneous dielectric in which a transmission line presents the same propagation constant of the corresponding microstrip line [11], and it is characterized by its effective electric permittivity  $\varepsilon_r^{\text{eff}} = (\varepsilon_r + 1)/2 + [(\varepsilon_r - 1)/2] \cdot [1 + 12(h_s/w_f)]^{-1/2}$ .

However, the effective electric permittivity depends on the frequency, and the dispersive effects represented by the loss tangent must be taken into account. It is accomplished by applying the multipole Debye model that describes the behavior of the complex electric permittivity in the frequency domain [12]:

$$\varepsilon_{eq} = \frac{2\varepsilon_r^{\text{eff}} \varepsilon_0}{k^{\frac{N-1}{2}} (k+1)} \left( 1 + \sum_{n=0}^{N-1} \frac{(k-1)k^n}{1 + \frac{j\omega k^{nm}}{\omega_0}} \right) \quad (5)$$

where  $m = \pi/2\delta$ , and  $k = 10^{1/m\varsigma}$  is the spacing factor related to the number  $\varsigma$  of elements per decade in the Debye model. The upper frequency bound  $\omega_0$  is related to the bandwidth center frequency as:  $\omega_0 = \omega_c 10^{\frac{N-1}{2\varsigma}}$ .

Therefore, the input parameters used in the implementation of the Debye model in this work are the effective electric permittivity  $\varepsilon_r^{\text{eff}}$ , the substrate loss tangent  $\tan \delta$ , the angular frequency  $\omega_c$  in which the substrate is characterized, the number  $\varsigma$  of substrate characterization samples, and the Debye model order  $N = 5$ , which assures a good accuracy for the entire analyzed frequency range.

### III. RESULTS

The formulation previously described was implemented in MATLAB. Moreover, from the current calculated through (1), it is possible to obtain electromagnetic parameters such as input impedance and near-field values as post-processing steps.

#### A. Experimental Validation

The input impedance can be calculated as  $Z_{in} = R_{in} + jX_{in} = V_S/I_S$ , where  $R_{in}$  and  $X_{in}$  are the input resistance and reactance,  $V_S$  is the input voltage, and  $I_S$  is the current along the segment connected to the source. Therefore, the input reactance  $X_{in}$  of the source coil is used to validate the proposed approach and its implementation. This choice was based on the fact that for an electrically small coil, i.e.  $L \ll \lambda$ ,  $X_{in} \gg R_{in}$ . Apart from that, due to the tolerance of commercial capacitors, it is convenient to validate first without any lumped elements.

Besides, the  $X_{in}$  of a coil with dimensions shown in Fig. 1(a) was measured with a Vector Network Analyzer (VNA). The calculated and measured results are shown in Fig. 2 for a frequency band from 1 MHz to 210 MHz. This broadband analysis allows us to validate the proposed approach in its full validity range since, at 1 MHz, the structure size corresponds to  $\lambda/1000$  whereas, at 210 MHz, it is  $\lambda/10$ , considering  $\lambda$  in free space.

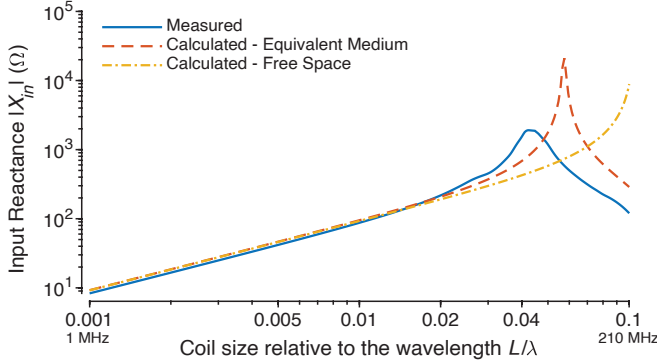


Fig. 2. Measured and calculated input reactance  $|X_{in}|$  of the source coil.

The results calculated with the proposed formulation agree with the measurements, particularly for frequencies in which  $L \geq \lambda/50$ . However, as the frequency increases, the structure size becomes comparable to the  $\lambda$  in the material medium, and the thin-wire approximation is no longer valid. Moreover, when the calculation considering the equivalent medium is compared to the results in free space, it is verified that the proposed formulation leads to a lower deviation in the resonant frequency. Since the dielectric medium increases the electrical length of the coil, its resonant frequency is consequently reduced. Therefore, the equivalent medium approach leads to more accurate results at frequencies closer to the validity limit of the thin-wire approximation.

#### B. Metasurface Performance

MTSs that support magnetic resonances can be characterized by their effective magnetic permeability  $\mu_{eff}$ . As the magnetic permeability of an inductor is proportional to its inductance,  $\mu_{eff}$  is given by the ratio between  $Z_{in}$  in the presence of the MTS:  $Z_{in}^{Coil+MTS} = R_{in}^{Coil+MTS} + j\omega X_{in}^{Coil+MTS}$

and the imaginary part of  $Z_{in}$  of the source coil alone  $jX_{in}^{Coil}$  [13]. Therefore,

$$\mu_{eff} = \Re(\mu_{eff}) - j\Im(\mu_{eff}) = \frac{X_{in}^{Coil+MTS}}{X_{in}^{Coil}} - j \frac{R_{in}^{Coil+MTS}}{X_{in}^{Coil}}. \quad (6)$$

The input impedance of the source coil was measured with ( $Z_{in}^{Coil+MTS}$ ) and without ( $Z_{in}^{Coil}$ ) the MTS. Then,  $\mu_{eff}$  was obtained by applying these measurements in Eq. (6). The measured and calculated  $\mu_{eff}$  are presented in Fig. 3.

The proposed formulation leads to accurate results for  $\Re(\mu_{eff})$ , particularly in the operating band of the MTS, i.e., around 12.3 to 13.3 MHz. However, regarding  $\Im(\mu_{eff})$ , even though the in-house code results well represent its behavior, there is a vertical offset between measured and calculated results. As  $\Im(\mu_{eff})$  represents the losses in the magnetic MTSs, this offset can be explained by the fact that physical capacitors have an Equivalent Series Resistance (ESR) that is not taken into account in the numerical formulation. However, if the ESR value is known, it can also be incorporated within  $Z_{load}$  in Eq. (3).

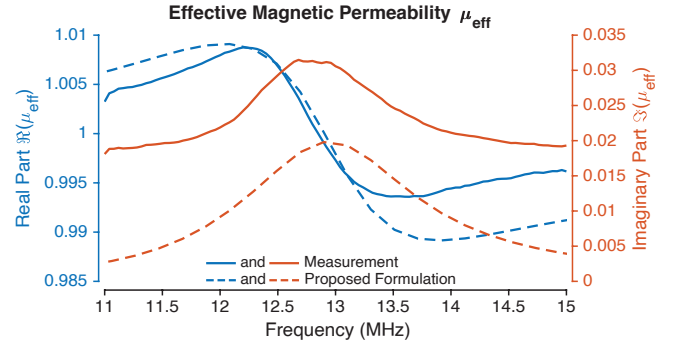


Fig. 3. Measured and calculated effective magnetic permeability  $\mu_{eff}$ .

The electromagnetic fields at any point in the space can be found from the current flowing in the structure [11]. Therefore, the magnetic flux density along the  $z$ -axis was calculated and measured in a distance range  $0 \leq d \leq 100$  mm from the center of the source coil.

The measurement setup is shown in Fig. 4. In this case, a 20 dBm sinusoidal signal at 12.6 MHz is applied to the source coil. Besides, a near-field loop probe with radius  $a = 17$  mm is aligned to the structure, and the received voltage  $V_L$  is measured for several positions. Finally, the magnetic flux density is found by  $|B_z| = V_L/(\omega\pi a^2)$  [11].

The magnetic flux density calculated using the proposed formulation and measured with the near-field probe is shown in Fig. 5. The calculated results agree with the measurement, with the most significant deviation at the MTS vicinity. This deviation is due to the fact that the losses in the physically realized MTS are higher than in the computed case, as previously discussed. Apart from that, the proposed formulation considers a homogeneous medium; therefore, the losses due to the reflections at the interface air-substrate are not taken into account. Nonetheless, the near-field amplification at the vicinity of the MTS is verified in the numerical results. However, the losses in the prototype attenuate this effect, making it less noticeable in the measurements.



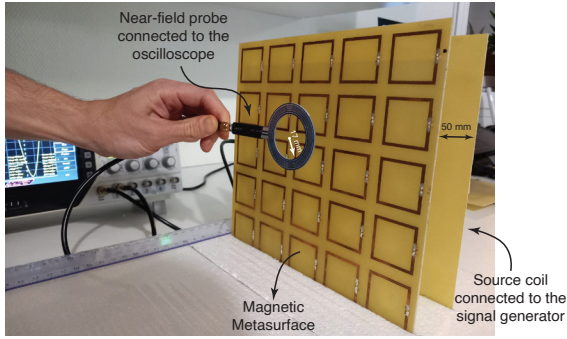


Fig. 4. Experimental setup to measure the magnetic flux density produced by the source coil in the presence of the magnetic MTS.

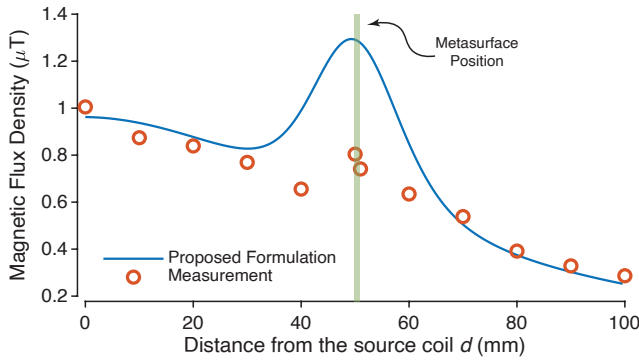


Fig. 5. Measured and calculated magnetic flux density.

### C. Wireless Power Transfer Efficiency

Finally, the WPT efficiency was calculated in two different cases. First, with a receiver identical to the source coil positioned at  $d = 100$  mm. Then, with the MTS inserted between them at  $d = 50$  mm. In both cases, the WPT efficiency is given by  $\eta = |S_{21}|^2$ , where  $S_{21}$  is the transmission coefficient from the source to the receiver coil.

Similarly,  $\eta$  was experimentally obtained for both cases by measuring  $S_{21}$  with the source and receiver coil connected to the VNA. The measured and calculated results at the operation frequency of 12.6 MHz are presented in Table I. As the source and receiver coils do not resonate in the operation frequency of the MTS, they are loosely coupled, which explains the low-efficiency values. However, even in this case, the inclusion of the MTS leads to an efficiency enhancement of about 35%.

TABLE I  
MEASURED AND CALCULATED WPT EFFICIENCY

WPT Efficiency	Proposed Formulation	Measured
Without Metasurface	$2.24 \times 10^{-3}$	$2.45 \times 10^{-3}$
With Metasurface	$3.4 \times 10^{-3}$	$3.3 \times 10^{-3}$

From the numerical perspective, the results calculated with the in-house code corroborate with the measured ones in both analyzed cases, confirming the feasibility of the proposed approach to analyze a complete WPT system with and without MTS. Apart from that, as only the conductor is discretized, there is a significant reduction in the computational cost compared to full-wave analysis using commercial software. Therefore, this formulation can also be used to speed up the design and optimization of WPT systems based on magnetic resonance.

## IV. CONCLUSION

The particular properties that arise from the interaction between the electromagnetic fields and the periodic structure of resonant MTS led to the development of novel devices. For instance, MTS is used to amplify the magnetic field, increasing the coupling between transmitter and receiver coils in an inductive WPT system. However, the analysis and synthesis of these structures are still computationally costly tasks.

Therefore, this paper proposed a novel approach that considers the dielectric loading effects on the thin-wire numerical formulation used to analyze microstrip devices. Besides, the results obtained from its implementation were compared with several experimental measurements. As a result, the proposed approach reproduces the behavior of a MTS and its effects on a WPT system. Moreover, as the dielectric properties are considered, it leads to more accurate results than previous results in the literature disregarding these effects.

For that reason, the proposed approach is suitable for analyzing complete WPT systems with and without MTS structures. Besides, it significantly reduces the computational cost compared to full-wave simulations since only the conductive structure is discretized. Consequently, it is a convenient tool to speed up the synthesis and optimization of magnetic resonators and WPT devices.

## ACKNOWLEDGMENT

This work was partially supported by FAPEMIG, CAPES, CNPq and CEFET-MG.

## REFERENCES

- [1] I. V. Soares and U. C. Resende, "Radially periodic metasurface lenses for magnetic field collimation in resonant wireless power transfer applications," *J. Microw. Optoelectron. Electromagn.*, vol. 21, no. 1, pp. 48–60, Mar. 2022.
- [2] G. Aiello, S. Alfonzetti, S. A. Rizzo, and N. Salerno, "Optimization of frequency selective surfaces for the design of electromagnetic mantle cloaks," *IEEE Trans. Magn.*, vol. 57, no. 6, pp. 1–4, 2021.
- [3] S. Sun, Q. He, J. Hao, S. Xiao, and L. Zhou, "Electromagnetic metasurfaces: physics and applications," *Adv. Opt. Photon.*, vol. 11, no. 2, pp. 380–479, Jun 2019.
- [4] X. Fan, F. Tang, B. Su, and X. Zhang, "Design of spiral resonator based on fractal metamaterials and its improvement for MCR-WPT performance," *IEEE Trans. Magn.*, vol. 58, no. 8, pp. 1–9, 2022.
- [5] H. Wang, W. Wang, X. Chen, Q. Li, and Z. Zhang, "Analysis and design of kHz-metamaterial for wireless power transfer," *IEEE Trans. Magn.*, vol. 56, no. 8, pp. 1–5, 2020.
- [6] Y. Otomo, Y. Sato, S. Fujita, and H. Igarashi, "Synthesis of equivalent circuit of wireless power transfer device using homogenization-based FEM," *IEEE Trans. Magn.*, vol. 54, no. 3, pp. 1–5, 2018.
- [7] L. Krähenbühl *et al.*, "Large surface LC-resonant metamaterials: From circuit model to modal theory and efficient numerical methods," *IEEE Trans. Magn.*, vol. 56, no. 2, pp. 1–4, 2020.
- [8] Z.-X. Wang, P.-C. Zhao, Z.-Y. Zong, W. Wu, and D.-G. Fang, "An extension of partial element equivalent circuit method for frequency selective surface analysis," *IEEE Trans. Antennas Propag.*, pp. 1–1, 2022.
- [9] W. Gibson, *The method of moments in electromagnetics*, 3rd ed. Boca Raton: Chapman and Hall/CRC, 2021.
- [10] A. F. Peterson, S. L. Ray, and R. Mittra, *Computational methods for electromagnetics*. Piscataway, New Jersey: IEEE Press, 1998.
- [11] C. Balanis, *Antenna theory: analysis and design*, 4th ed. Hoboken, New Jersey: Wiley, 2016.
- [12] A. E. Engin, I. Ndip, K.-D. Lang, and J. Aguirre, "Closed-form multipole debye model for time-domain modeling of lossy dielectrics," *IEEE Trans. Electromagn. Compat.*, vol. 61, no. 3, pp. 966–968, 2019.
- [13] D. Ahn, M. Kiani, and M. Ghovanloo, "Enhanced wireless power transmission using strong paramagnetic response," *IEEE Trans. Magn.*, vol. 50, no. 3, pp. 96–103, 2014.